



Novel (Na, O) co-doped $\text{g-C}_3\text{N}_4$ with simultaneously enhanced absorption and narrowed bandgap for highly efficient hydrogen evolution

Wenjian Fang, Junying Liu, Lei Yu, Zhi Jiang, Wenfeng Shangguan*

Research Center for Combustion and Environment Technology, Shanghai Jiao Tong University, Shanghai 200240, China



ARTICLE INFO

Article history:

Received 19 February 2017
Received in revised form 7 March 2017
Accepted 15 March 2017
Available online 18 March 2017

Keywords:

$\text{g-C}_3\text{N}_4$
Photocatalytic hydrogen evolution
Co-doping
Solvothermal method

ABSTRACT

The photocatalytic activity of bulk $\text{g-C}_3\text{N}_4$ is rather low. Many strategies have been adopted to improve the photocatalytic performance of $\text{g-C}_3\text{N}_4$. Here, Na and O co-doped $\text{g-C}_3\text{N}_4$ was prepared by a feasible solvothermal method. The band structure was modulated mainly by introducing O into lattice of $\text{g-C}_3\text{N}_4$, resulting in simultaneously enhanced absorption and red shift. Moreover, the separation and migration of photogenerated carriers under visible light was enhanced by Na doping. In addition, well dispersion of (Na, O)- $\text{g-C}_3\text{N}_4$ in pure water was observed due to its high surface electronegativity. The photocatalytic H_2 production activity of (Na, O)- $\text{g-C}_3\text{N}_4$ was improved tremendously, especially under visible light, and the apparent quantum yield was as high as 22.3% at 420 nm.

© 2017 Elsevier B.V. All rights reserved.

1. Introduction

Since Graphitic Carbon Nitride ($\text{g-C}_3\text{N}_4$) was firstly found to be capable for the water-reduction and water-oxidation half reaction under visible light irradiation ($\lambda > 420 \text{ nm}$) [1], it attracts much attention worldwide. It has been applied in water splitting [2], organic pollution degradation [3] and CO_2 reduction [4], due to its suitable band positions and chemical stability. However, the photocatalytic activity of bulk $\text{g-C}_3\text{N}_4$ is rather low. The main reasons are the large optical band gap, low light absorption and the high recombination rate of photogenerated electron-hole pairs. To improve the photocatalytic performance of $\text{g-C}_3\text{N}_4$, many strategies have been adopted. Including: 1) increase visible light absorption by doping foreign elements such as oxygen [5,6], sulphur [7,8], phosphorous [9], fluorine [10], or both boron and fluorine [11] into the $\text{g-C}_3\text{N}_4$. 2) promote the separation of photogenerated electron-hole pairs by surface functionalization [12–14] or coupling $\text{g-C}_3\text{N}_4$ with another semiconductor [15–22]. 3) increase specific surface area by the introduction of mesoporous $\text{g-C}_3\text{N}_4$ [23]. 4) shorten the photogenerated electron-hole mobility distance by exfoliated $\text{g-C}_3\text{N}_4$ [24–27].

Usually, bulk $\text{g-C}_3\text{N}_4$ is synthesized by the polycondensation of various organic precursors containing both carbon and nitrogen

such as cyanamide, melamine, and other *s*-triazine heterocyclic compounds. However, this bulk condensation suffers from many problems, such as small specific surface area, low crystallinity and uncontrollable structure and morphology, which may result in high recombination rate and weak light absorptivity. In addition, bulk $\text{g-C}_3\text{N}_4$ prepared by the polycondensation of urea usually has larger optical band gap than other organic precursors [28]. Thus, $\text{g-C}_3\text{N}_4$ prepared by polycondensation needs to be modified for improving the photocatalytic activity. In general, there are two ways to modify $\text{g-C}_3\text{N}_4$: the top-down fabrication and the bottom-top fabrication. Now, the top-down fabrication is to change bulk $\text{g-C}_3\text{N}_4$ by ultrasound exfoliation [24] or liquid exfoliation [25,29] routes. While the bottom-top fabrication is to change precursors and reaction condition of polycondensation. For example, $\text{g-C}_3\text{N}_4$ can be prepared directly by polycondensation of precursors mixing with metal or nonmetal ions [30,31]. Polycondensation of precursors in a molten salt medium is claimed to produce crystalline graphitic CN [32]. Moreover, soft solution processing methods to assemble large polymeric superstructures at low temperature are explored [33].

Here, we introduce a top-down fabrication to modify the bulk $\text{g-C}_3\text{N}_4$ prepared by the polycondensation of urea. A novel crystalline (Na, O) co-doped $\text{g-C}_3\text{N}_4$ is successfully obtained. The photocatalytic H_2 production activity of the sample as prepared is improved tremendously due to its narrowed bandgap, increased light absorptivity and well dispersion.

* Corresponding author.

E-mail address: shangguan@sjtu.edu.cn (W. Shangguan).

2. Experimental methods

Urea (>99.0%), Ethanol (99.7%), NaOH (>96%) and $H_2PtCl_6 \cdot 6H_2O$ were purchased from Sinopharm Chemical Reagent Co., Ltd., (China). Doubly distilled water was used throughout this work. All other reagents were of analytical reagent grade, without further purification.

2.1. Preparation of bulk- $g\text{-}C_3N_4$

The photocatalyst of $g\text{-}C_3N_4$ was prepared by heating urea to 873 K in an alumina crucible with aluminum foil as a cover. The heating rate was 2.5 K/min. When cooling to room temperature naturally, the $g\text{-}C_3N_4$ was got without further treatment. It was named bulk $g\text{-}C_3N_4$.

2.2. Preparation of $(Na, O)\text{-}g\text{-}C_3N_4$

Then as-prepared bulk $g\text{-}C_3N_4$ (0.5 g) was suspended in 60 ml ethyl alcohol with 0.5 g sodium hydroxide added. After vigorous stirring for 1 h, the suspension was transferred into a 100 ml stainless Teflon-lined autoclave. The autoclave was heated at 433 K for 10 h and then cooled down to room temperature naturally. The resulting yellow precipitates were subjected to 20 min of centrifugation at 10000 rpm with distilled water several times until the pH = 7. The light yellow colloidal solution was collected. And the remained precipitates were dried at 353 K in air overnight. It was named $(Na, O)\text{-}g\text{-}C_3N_4$.

2.3. Photo-deposition Pt

The cocatalysts were loaded by *situ* photo-deposition method [1]. 0.05 g $(Na, O)\text{-}g\text{-}C_3N_4$ as prepared was suspended in 60 ml deionized water and 20 ml ethyl alcohol with ultrasound for 20 min in a Pyrex reaction cell. Then H_2PtCl_6 solution (0.004 g/ml) containing 1 mg Pt was added to the mixed solution above. The suspension was thoroughly degassed and irradiated by Xe lamp for 3 h. After that, the grey sediment was filtered, and dried at 353 K in air for overnight.

2.4. Photocatalytic tests

The photocatalytic reactions were carried out in a Pyrex reaction cell connected to a closed gas circulation and evacuation system. Typically, 0.05 g $g\text{-}C_3N_4$ with Pt as co-catalyst was suspended in 60 ml deionized water and 20 ml ethyl alcohol. Then the suspension was thoroughly degassed and irradiated by a Xe lamp (300 W) equipped with an optical cutoff filter ($\lambda > 400$ nm, containing 1 M $NaNO_2$, transmittance showed in Fig. S1). The amount of H_2 was analyzed every hour using an online gas chromatography.

2.5. Materials characterization

XRD patterns were tested on a D8 DA VINCE (Bruker) X-ray diffractometer using a $Cu K\alpha$ ray radiation source. The scanning speed was 6°/min, tube voltage was 40 kV, and tube current was 40 mA. The UV-vis diffuse reflection spectra (DRS) were determined by a UV-vis spectrophotometer UV-2450 (Shimadzu, Japan) and were converted to absorbance by the Kubelka–Munkmethod. The morphology of the products was investigated by SEM (JEOL JSM-6380LV) and transmission electronic micrograph (TEM, JEM-2010, operated at 200 kV). Fourier transformed infrared (FTIR) spectra were recorded on Nicolet6700 Spectrometer. The XPS patterns were measured on an AXIS UltraDLD electronic energy spectrum (Kratos group) at 300 W using $Mg K\alpha$ X-rays as the excitation source. The binding energies (BE) of the elements were

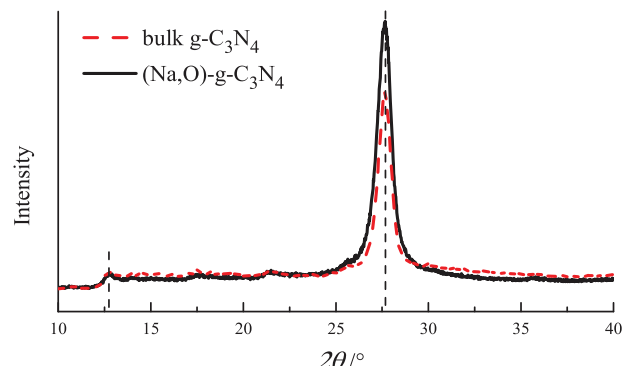


Fig. 1. XRD patterns of bulk $g\text{-}C_3N_4$ and $(Na, O)\text{-}g\text{-}C_3N_4$.

calibrated relative to the carbon impurity with a C 1s at 284.8 eV. Zeta potential analysis was examined by Zetasizer Nano ZSP. The concentration of elements was analysed using Inductively Coupled Plasma Atomic Emission Spectrometry (ICP-AES, Thermo-iCAP6300).

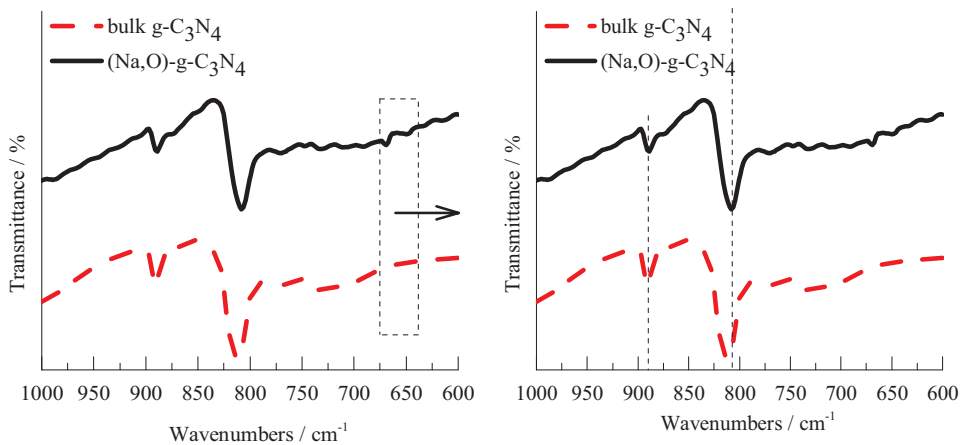
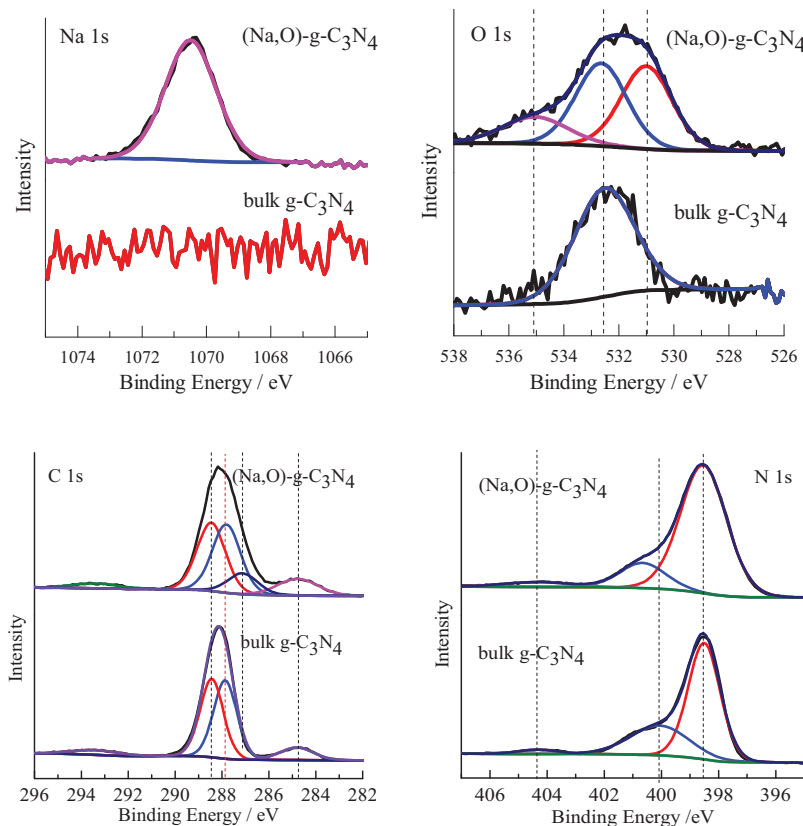
3. Results and discussion

To study the synthesis mechanism of $(Na, O)\text{-}g\text{-}C_3N_4$, a series experiments have been done. Bulk $g\text{-}C_3N_4$ has no obvious change after solvothermal treatment with only adding ethyl alcohol or water, while nothing sediment is obtained with adding sodium hydroxide and water simultaneously (see Table S2). It suggests that bulk $g\text{-}C_3N_4$ can be decomposed in alkaline solution by hydrothermal methods. The XRD of the product $(Na, O)\text{-}g\text{-}C_3N_4$ is given in Fig. 1. The strongest XRD peak at 27.65°, due to the stacking of the conjugated aromatic system, is enhanced by hydrothermal method. It suggests that the crystal structure of $g\text{-}C_3N_4$ is not changed, and the crystallinity of $g\text{-}C_3N_4$ along (002) planes is increased during hydrothermal process.

FTIR spectra are shown in Fig. 2. The peaks 3500–3000 cm^{-1} originating from the N–H stretches and peaks 1700–1000 cm^{-1} corresponding to the characteristic stretching modes of C–N and C=N, are nearly the same between the bulk $g\text{-}C_3N_4$ and $(Na, O)\text{-}g\text{-}C_3N_4$ [24]. Thus, the chemical structures of $(Na, O)\text{-}g\text{-}C_3N_4$ is similar to that of the bulk $g\text{-}C_3N_4$ after hydrothermal method. However, there is a distinct peak shifting from 813 cm^{-1} to 807 cm^{-1} . The peak at 813 cm^{-1} belongs to out of plane bending of trisubstituted tri-s-triazine ring [34]. The red-shifted of condensed CN heterocycles vibration frequencies suggests the enhancement of conjugate effect. We think it is caused by increased crystallinity of $g\text{-}C_3N_4$ along (002) planes and the O doping.

The chemical bonding between the component elements on the surface of $g\text{-}C_3N_4$ is investigated by the X-ray photoelectron spectroscopic (XPS) measurements. The high-resolution C1s, N1s, O1s and Na1s spectra of both $(Na, O)\text{-}g\text{-}C_3N_4$ and bulk $g\text{-}C_3N_4$ are given in Fig. 3. In their C1s spectra, a peak located at 284.8 eV is typically ascribed to graphitic C–C. Moreover, the peak centered at the 288.1 eV is further deconvoluted into two Gaussian–Lorentzian peaks located at 287.8 eV and 288.5 eV. The first one is attributed to the sp² hybridized N–C=N inside the triazine rings, while the other is assigned to the sp² hybridized C–NH₂ groups. Besides peaks in common above, the $(Na, O)\text{-}g\text{-}C_3N_4$ shows a new-generated peak at 287.2 eV which is ascribed to the C–O bond [8].

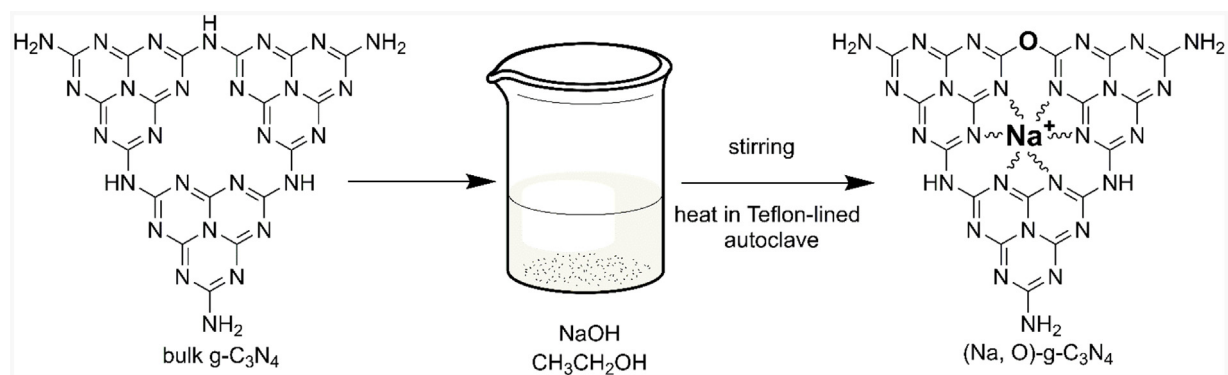
The high-resolution N1s spectra can be deconvoluted into three different peaks at binding energies of 398.5 eV, 400.6 eV, and 404.5 eV. The peak at 398.5 eV corresponds to the sp² hybridized C=N–C involved in the triazine rings, while the peak at 400.6 eV is attributed to the bridging N atoms in N–(C)₃ or C–NH₂. It is thought the obvious shifting for peak at 400.6 eV is caused by N–C–O

Fig. 2. FTIR spectra of bulk $\text{g-C}_3\text{N}_4$ and $(\text{Na}, \text{O})\text{-g-C}_3\text{N}_4$.Fig. 3. XPS survey spectra of bulk $\text{g-C}_3\text{N}_4$ and $(\text{Na}, \text{O})\text{-g-C}_3\text{N}_4$.

species. Moreover, the weak peak at 404.5 eV can be assigned to can be assigned to π -excitations [8,24].

The high-resolution O1s and Na1s spectra provide a direct evidence of (O, Na) co-doping into bulk $\text{g-C}_3\text{N}_4$ (Fig. 3). O1s of the bulk $\text{g-C}_3\text{N}_4$ has only one peak centered at 532.6 eV which ascribed to adsorbed water. On the other hand, another two distinct peaks located at 531 eV and 535.1 eV are detected on the $(\text{Na}, \text{O})\text{-g-C}_3\text{N}_4$. They can be attributed to the formation of N—C—O species and the adsorbed O_2 , respectively [5]. Furthermore, The Na1s peaks of $(\text{Na}, \text{O})\text{-g-C}_3\text{N}_4$ are discovered at 1070.3 eV, which is lower than that of any sodium salt [30,35]. We think that the Na ions are coordinated into the big C—N rings formed by the N-bridge linking of the

triazine units in the plane of $\text{g-C}_3\text{N}_4$ (see Scheme 1). Firstly, the calculation result of surface elemental concentration determined by XPS reveals that the $(\text{Na}, \text{O})\text{-g-C}_3\text{N}_4$ is 2.75 wt%, which is very close to the ICP result (2.64 wt%). If Na ions are mainly adsorbed on the surface of the $\text{g-C}_3\text{N}_4$, the XPS result should be much higher than that of ICP result. Therefore, it proves that Na should be doped into the $\text{g-C}_3\text{N}_4$ lattice uniformly during the hydrothermal process [35]. Secondly, the binding energy of $(\text{Na}, \text{O})\text{-g-C}_3\text{N}_4$ is 1070.3 eV in the Na 1s region which obviously lower than that of any sodium salt as well as Na—O group. In addition, the atomic radius of C and N (70 and 65 pm) is much smaller than that of Na^+ (about 100 pm). So, Na could not be doped as an ion state in a substitutional site.



Scheme 1. Scheme of (Na, O) co-doped g-C₃N₄ obtained by solvothermal method.

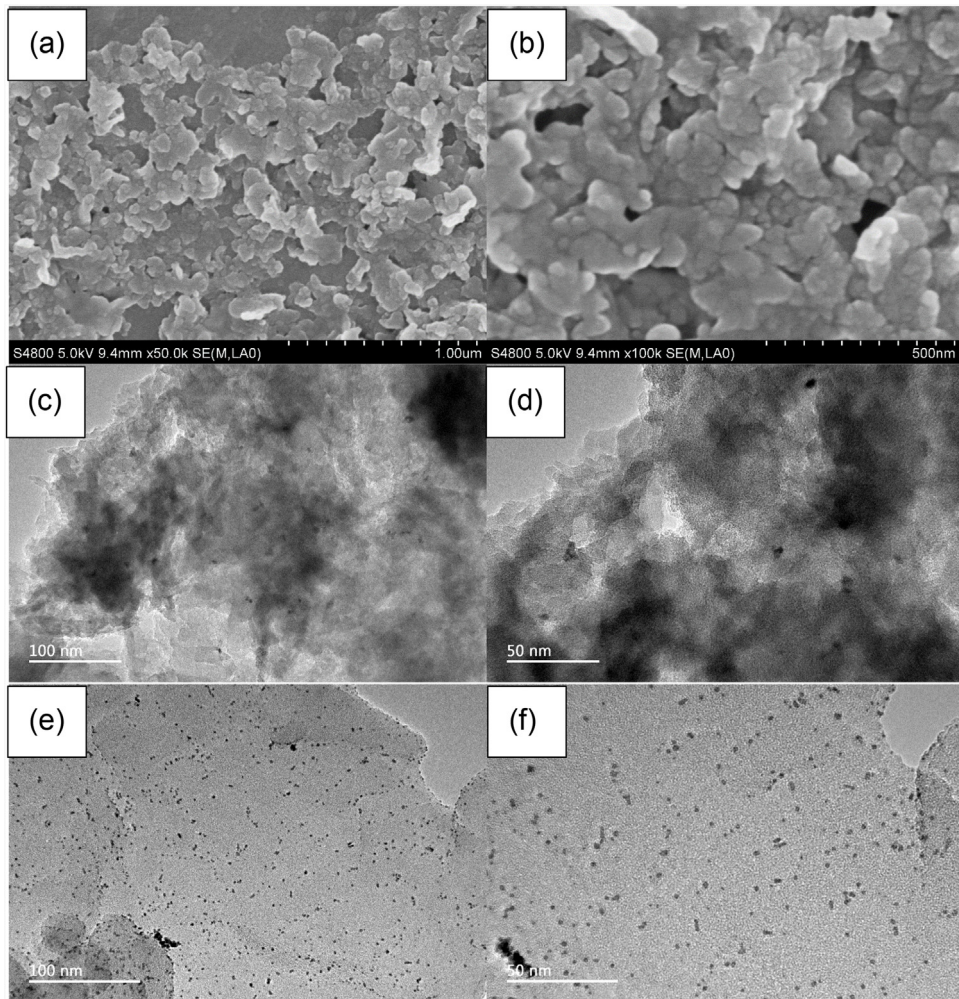


Fig. 4. Typical FE-SEM and TEM of (Na, O)-g-C₃N₄ (a–d); TEM of bulk g-C₃N₄ (e–f).

It confirms that the Na ions are coordinated into the big C—N rings formed by the N—bridge linking of the triazine units in the plane of g-C₃N₄. Thirdly, it is confused that peak shifting at 27.65° of (Na, O)-g-C₃N₄ is not observed from XRD spectra (see Fig. 1). As we know, the peak at 27.65° of the O-doped g-C₃N₄ will shift to a larger 2θ corresponding to a decrease in the interplanar [5]. Instead, this peak of the Na-doped g-C₃N₄ will shift to a lower 2θ value due to enlarged the interlayer spacing [35]. Thus, peak shifting at 27.65° of (Na, O)-

g-C₃N₄ is not observed. In short, the Na ions are coordinated into the big C—N rings formed by the N—bridge linking of the triazine units in the plane of g-C₃N₄ and O is mainly in a substitutional site for N.

Morphology of the as-prepared (Na, O)-g-C₃N₄ powder sample are observed by FE-SEM and TEM (Fig. 4). (Na, O)-g-C₃N₄ composes a number of irregular particles with the layered structure. Especially, bulk g-C₃N₄ looks more transparent than (Na, O)-g-C₃N₄.

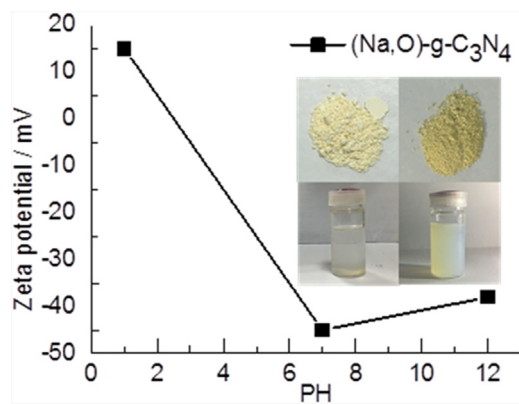


Fig. 5. Zeta potential of (Na, O)-g-C₃N₄ at different pH values. Inset images: (a) Photographs of powders; (b) Photographs of samples dispersed in pure water after being stored for two months under ambient conditions. (left: bulk g-C₃N₄; right: (Na, O)-g-C₃N₄).

from TEM. So (Na, O)-g-C₃N₄ has a more compact structure than bulk g-C₃N₄ which is consistent with the XRD results. The strongest XRD peak at 27.65°, due to the stacking of the conjugated aromatic system, is enhanced. It suggests that the crystallinity of (Na, O)-g-C₃N₄ along (002) planes is increased. In macroscopic view, the powder of bulk g-C₃N₄ is rather fluffy while (Na, O)-g-C₃N₄ compact (see Fig. 5a). Moreover, due to the doping of alkali metal ions, the surface of (Na, O)-g-C₃N₄ will have a strong electronegativity at pH=7 (Fig. 5) [36]. Both the nanosheets and surface electronegativity lead to high dispersion of (Na, O)-g-C₃N₄ in pure water. From Fig. 5b, no sediment of (Na, O)-g-C₃N₄ colloidal dispersion is observed after being stored for 2 months under ambient conditions.

From the analysis of the crystal structure, chemical structures, and surface bonding states, it is concluded that crystallinity (Na, O) co-doped g-C₃N₄ is successfully prepared by hydrothermal method. The optical properties have been further investigated by UV-vis diffuse reflectance spectra. From Fig. 6a, it is found that the absorption edge of (Na, O)-g-C₃N₄ shows a remarkable red shift from about 420–460 nm. Moreover, the bandgap speculated by using the Tauc equation decreases from 2.96 eV to 2.72 eV compared with that of bulk g-C₃N₄. Surprisingly, (Na, O)-g-C₃N₄ has apparently enhanced absorption of both the UV and visible light. The decreased bandgap is mainly contributed by O doping [5,30]. As the doped O 2p orbitals have a lower potential than the N 2p orbitals, the VBM of the bulk g-C₃N₄ will not be changed by the introduction of oxygen atoms. Since the substitution of N sites by O atoms, the extra electrons would be redistributed to their nearest carbon atoms and delocalized among the big π bonds of the

(Na, O)-g-C₃N₄. Thus, a defect-related state below the CBM of the g-C₃N₄ will be formed [22]. Moreover, enhanced absorption of UV is mainly due to the increased crystallinity.

The photocatalytic H₂ production activities of bulk g-C₃N₄ and (Na, O)-g-C₃N₄ are shown in Fig. 6b. The H₂ production rate is 16 $\mu\text{mol}/\text{h}$ and 110 $\mu\text{mol}/\text{h}$ under Xe lamp, respectively. Moreover, with NaNO₂ filter, the H₂ production rate of (Na, O)-g-C₃N₄ is about 45 $\mu\text{mol}/\text{h}$, while bulk g-C₃N₄ has little H₂ production. For comparison with the precious published papers, we also use TEOA as sacrifice agent to measure the apparent quantum efficiency [1,27]. The average H₂ production rate is about 810 $\mu\text{mol}/\text{h}$ under Xe lamp with TEOA as sacrifice agent and Pt (1 wt%) as co-catalyst. Bubbles can be observed obviously without stirring (see Fig. S3). The apparent quantum efficiency at 420 nm is about 22.3% which is fairly higher than the precious published papers [5,6,31,35].

We think both O and Na make contributions to the enhancing photocatalytic activity. Though single O doped g-C₃N₄ and Na doped g-C₃N₄ have been reported previously, both of them attend to one thing and lose another. For example, O doped g-C₃N₄ has a larger absorb edge with unimproved separation and migration of photogenerated carriers [5], while Na doped g-C₃N₄ reduce the recombination of photogenerated carriers with nearly unchanged bandgap [30]. Thus, O and Na co-doped g-C₃N₄ will inherit their advantages to improve photocatalytic activity tremendously. From the analysis above, the reasons for improved photocatalytic activity of (Na, O)-g-C₃N₄ are summarized below: 1) the increased absorption of both the UV and visible light; 2) fast separation and migration of photogenerated carriers by Na [30]; 3) high dispersion in pure water caused by strong surface electronegativity.

4. Conclusions

In summary, we introduce a new simple method to modify bulk g-C₃N₄ with enhanced photocatalytic activity. High crystalline and dispersive (Na, O) co-doped g-C₃N₄ can be prepared by hydrothermal method. The bandgap decreases from 2.96 eV to 2.72 eV compared with that of bulk g-C₃N₄. Moreover, obviously enhanced absorption of both the UV and visible light is observed. The photocatalytic H₂ production activity is improved about seven times compared with bulk g-C₃N₄.

Acknowledgements

We thank the National Natural Science Foundation of China (20973110, 21577088) and the National Key Basic Research and Development Program (2009CN220000) for the financial support.

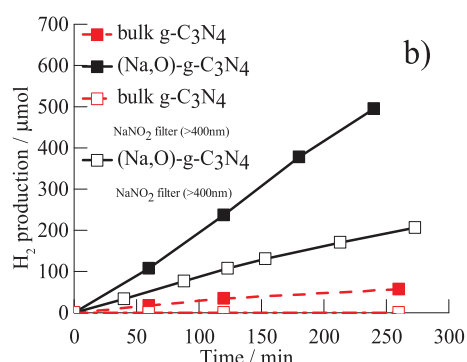
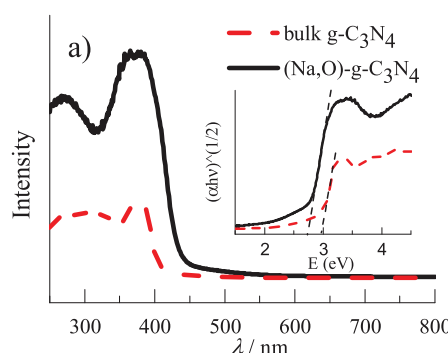


Fig. 6. (a) UV-vis absorption spectra of bulk g-C₃N₄ and (Na, O)-g-C₃N₄; (b) the photocatalytic H₂-production activity of bulk g-C₃N₄ and (Na, O)-g-C₃N₄ under Xe lamp with ethyl alcohol as sacrifice agent and Pt (2 wt%) co-catalyst.

Appendix A. Supplementary data

Supplementary data associated with this article can be found, in the online version, at <http://dx.doi.org/10.1016/j.apcatb.2017.03.041>.

References

- [1] X. Wang, K. Maeda, A. Thomas, K. Takanabe, G. Xin, J.M. Carlsson, K. Domen, M. Antonietti, *Nat. Mater.* 8 (2009) 76–80.
- [2] J. Liu, Y. Liu, N. Liu, Y. Han, X. Zhang, H. Huang, Y. Lifshitz, S.T. Lee, J. Zhong, Z. Kang, *Science* 347 (2015) 970–974.
- [3] S.C. Yan, Z.S. Li, Z.G. Zou, *Langmuir* 26 (2010) 3894–3901.
- [4] H. Shi, G. Chen, C. Zhang, Z. Zou, *ACS Catal.* 4 (2014) 3637–3643.
- [5] J. Li, B. Shen, Z. Hong, B. Lin, B. Gao, Y. Chen, *Chem. Commun.* 48 (2012) 12017–12019.
- [6] X. She, J. Wu, J. Zhong, H. Xu, Y. Yang, R. Vajtai, J. Lou, Y. Liu, D. Du, H. Li, P.M. Ajayan, *Nano Energy* 27 (2016) 138–146.
- [7] G. Liu, P. Niu, C. Sun, S.C. Smith, Z. Chen, G.Q. Lu, H.M. Cheng, *J. Am. Chem. Soc.* 132 (2010) 11642–11648.
- [8] M. Seredych, S. Loś, D.A. Giannakoudakis, E. Rodríguezcastellón, T.J. Bandosz, *ChemSusChem* 9 (2016) 795–799.
- [9] Y. Zhang, T. Mori, J. Ye, M. Antonietti, *J. Am. Chem. Soc.* 132 (2010) 6294–6295.
- [10] Y. Wang, Y. Di, M. Antonietti, H. Li, X. Chen, X. Wang, *Chem. Mater.* 22 (2010) 5119–5121.
- [11] Y. Wang, J. Zhang, X. Wang, M. Antonietti, H. Li, *Angew. Chem. Int. Ed.* 49 (2010) 3356–3359.
- [12] Y. Guo, S. Chu, S. Yan, Y. Wang, Z. Zou, *Chem. Commun.* 46 (2010) 7325–7327.
- [13] M. Zhang, W. Yao, Y. Lv, X. Bai, Y. Liu, W. Jiang, Y. Zhu, *J. Mater. Chem. A* 2 (2014) 11432.
- [14] X. She, J. Wu, H. Xu, Z. Mo, J. Lian, Y. Song, L. Liu, D. Du, H. Li, *Appl. Catal. B: Environ.* 202 (2017) 112–117.
- [15] R.C. Pawar, S. Kang, S.H. Ahn, C.S. Lee, *RSC Adv.* 5 (2015) 24281–24292.
- [16] Q. Nong, M. Cui, H. Lin, L. Zhao, Y. He, *RSC Adv.* 5 (2015) 27933–27939.
- [17] Y. He, L. Zhang, M. Fan, X. Wang, M.L. Walbridge, Q. Nong, Y. Wu, L. Zhao, *Sol. Energy Mater. Sol. Cells* 137 (2015) 175–184.
- [18] K. Dai, L. Lu, C. Liang, G. Zhu, Q. Liu, L. Geng, J. He, *Dalton Trans.* 44 (2015) 7903–7910.
- [19] S.-W. Cao, X.-F. Liu, Y.-P. Yuan, Z.-Y. Zhang, Y.-S. Liao, J. Fang, S.C.J. Loo, T.C. Sum, C. Xue, *Appl. Catal. B* 147 (2014) 940–946.
- [20] Y. Ji, J. Cao, L. Jiang, Y. Zhang, Z. Yi, *J. Alloys Compd.* 590 (2014) 9–14.
- [21] J. Zhang, Y. Wang, J. Jin, J. Zhang, Z. Lin, F. Huang, J. Yu, *ACS Appl. Mater. Interfaces* 5 (2013) 10317–10324.
- [22] X.H. Li, J.S. Chen, X. Wang, J. Sun, M. Antonietti, *J. Am. Chem. Soc.* 133 (2011) 8074–8077.
- [23] X. Wang, K. Maeda, X. Chen, K. Takanabe, K. Domen, Y. Hou, X. Fu, M. Antonietti, *J. Am. Chem. Soc.* 131 (2009) 1680–1681.
- [24] S. Yang, Y. Gong, J. Zhang, L. Zhan, L. Ma, Z. Fang, R. Vajtai, X. Wang, P.M. Ajayan, *Adv. Mater.* 25 (2013) 2452–2456.
- [25] J. Xu, L. Zhang, R. Shi, Y. Zhu, *J. Mater. Chem. A* 1 (2013) 14766.
- [26] X. Zhang, X. Xie, H. Wang, J. Zhang, B. Pan, Y. Xie, *J. Am. Chem. Soc.* 135 (2013) 18–21.
- [27] G. Liu, T. Wang, H. Zhang, X. Meng, D. Hao, K. Chang, P. Li, T. Kako, J. Ye, *Angew. Chem. Int. Ed.* 54 (2015) 13561–13565.
- [28] D.J. Martin, K. Qiu, S.A. Shevlin, A.D. Handoko, X. Chen, Z. Guo, J. Tang, *Angew. Chem. Int. Ed.* 126 (2014) 9394–9399.
- [29] X. She, L. Liu, H. Ji, Z. Mo, Y. Li, L. Huang, D. Du, H. Xu, H. Li, *Appl. Catal. B: Environ.* 187 (2016) 144–153.
- [30] M. Zhang, X. Bai, D. Liu, J. Wang, Y. Zhu, *Appl. Catal. B* 164 (2015) 77–81.
- [31] M. Wu, J.M. Yan, X.N. Tang, M. Zhao, Q. Jiang, *ChemSusChem* 7 (2014) 2654–2658.
- [32] Y. Ham, K. Maeda, D. Cha, K. Takanabe, K. Domen, *Chem. Asian J.* 8 (2013) 218–224.
- [33] Y. Cui, Z. Ding, X. Fu, X. Wang, *Angew. Chem. Int. Ed.* 51 (2012) 11814–11818.
- [34] R.C. Dante, P. Martín-Ramos, A. Correa-Guimaraes, J. Martín-Gil, J. Martín-Gil, *Mater. Chem. Phys.* 130 (2011) 1094–1102.
- [35] J. Zhang, S. Hu, Y. Wang, J. Martín-Gil, *RSC Adv.* 4 (2014) 62912–62919.
- [36] K. Schwinghamer, M.B. Mesch, V. Duppel, C. Ziegler, J. Senker, B.V. Lotsch, *J. Am. Chem. Soc.* 136 (2014) 1730–1733.